Memo

To
Arjan Sieben

Date
27 December 2011

Number of pages
14

From
Sanjay Giri

Direct line
+31 (0)88 33 58 471

E-mail
sanjay.giri@deltares.nl

Subject
Implementation of dune orientation in Delft3D: Additional study
Case studies with slope effect including Talmon's correction

Copy for
Arno Talmon, Kees Sloff

1 Background

The following issues have been investigated herein:

1) Computation of the angle of dune orientation (α): The equation for the angle of dune orientation (based on Sieben & Talmon, 2011) has been solved and implemented in Delft3D code. The details of the approach can be found in previous memos.

2) Three different approaches have been used to solve the equation, namely predictor-corrector, iterative with an additional transient term and the bisection method.

3) Case studies with the slope effect including Talmon's correction (consideration of relative grain-size) and comparison with the conventional DVR approach, in which the relative grain-size were not taken into account although the slope effect parameters (A_{shd} and B_{shd}) were adapted/calibrated for each calculation domain.

4) Case studies have been carried out for the Waal as well as IJssel models.

2 Computations

2.1 Model tests for the angle of dune orientation (implemented in Delft3D open source)

2.1.1 Model schematization

Two models have been schematized, namely a narrow straight channel with side slopes, and a curved flume.

The channel cross-section for the straight flume is depicted in Figure 1; the curved channel configuration can be seen in Figure 2.

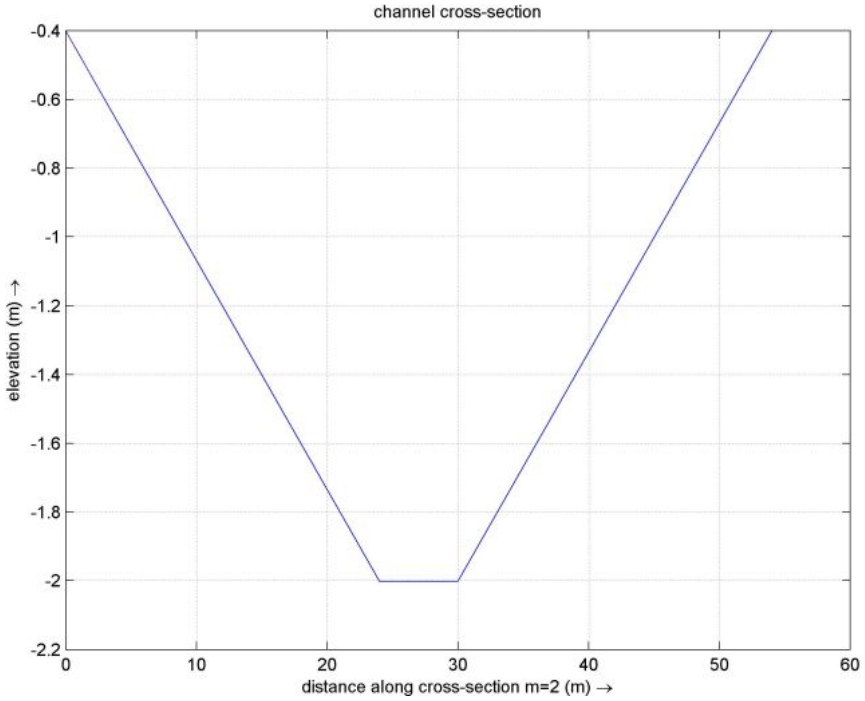

Figure 1 Channel cross-section for straight channel

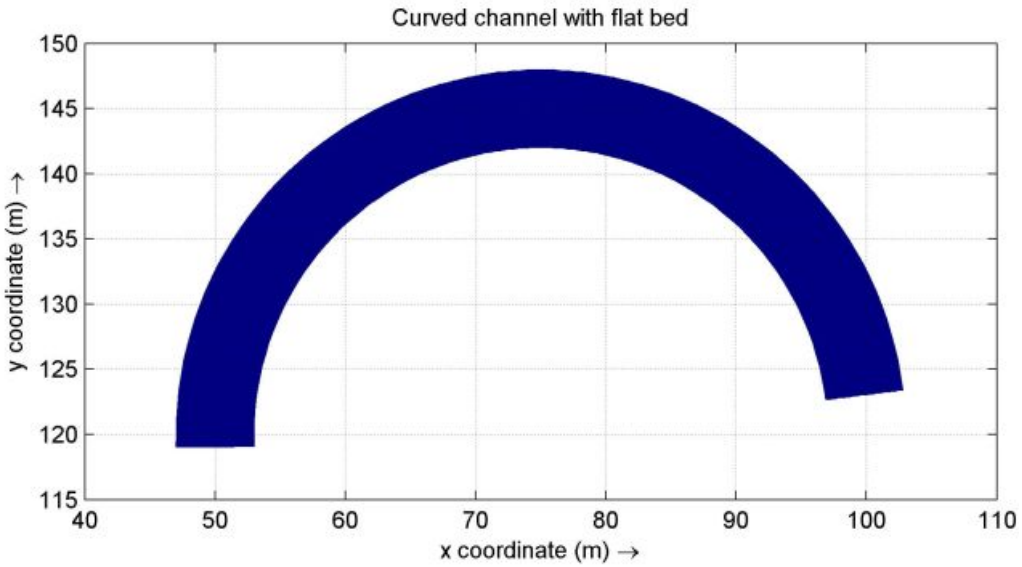

Figure 2 Curved channel with flat bet

2.1.2 Computational results

As it has been mentioned above, three schemes for solving the equation have been incorporated. We have also checked the direction of dune orientation and it's consistency with the transverse gradient of dune migration (this was a problem in our previous studies).

As can be seen from the results (Figure 3 - Figure 7), all schemes provide identical results for both curved as well as straight channels, which give us a confidence on the correctness of the solution. For these ideal cases, the difference in solution schemes does not seem to be obvious. However, this might be important in case we use more complex models (as during our offline tests, we found that for a certain input parameters, the convergence might be an issue and the performance of each scheme).

Furthermore, it can be concluded that the sign of dune orientation is correct, e.g. for the curved channel, the sign is > 0 (Figure 3), which implies that the dune orientation is towards the outer bend. This is consistent with the result for the migration speed (Figure 4) that shows the dune is moving faster at the inner bend. The similar result can be found for the straight flume (Figure 6 - Figure 7), in which it can be seen that the dune migration rate is higher near the bank (except for the near-boundary cells!) and low in the middle, which implies that the dune angle is positive in the right part of the channel and negative in the left part. This is more evident in one of the plotting for a selected cross-section (Figure 8).

2.1.3 Preliminary conclusion

The dune orientation, computed by using different solvers, appears to be correct in terms of both magnitude and direction. The main issue remains to be checked is the convergence of the solution for the real-world application and its performance in case there is local problems (e.g. high gradients in some local quantities that are in the equation). In this connection, some offline analyses have been done, and the report will be prepared in near future. Furthermore, the approach has to be tested, for instance, with the Waal model before implementing the feedback to sediment transport (although, the grid of the Waal, being used for the DVR model, might not be appropriate for this check). Nevertheless, the feedback to the sediment transport and its effect will be tested in near future.

2.2 Case studies for the slope effect considering relative grain-size (Talmon's correction)

In DVR model, the effect of relative grain-size on correction of sediment transport direction was always neglected (although, the parameters A_{shd} and B_{shd} were calibrated for each domain that somehow appears to be compensating the negligence of relative grain-size).
Herein, we have incorporated the relative grain-size term in the slope correction parameter and compare the outcomes, based on the case studies with the Waal and the IJssel models.

So, the following relation for $f(\theta)$ is used:

$$f(\theta) = A_{shd}\, \theta^{Bshd}\, (d_{50}/h)^{Cshd} \qquad (1)$$

2.2.1 Case study for the Waal model

The values for the parameters for the Waal models:

In reference computation (referred to as DVR approach): A_{shd} =0.7; B_{shd}=0.5 and C_{shd}=0 for all three domains (E_{spir} = 1.0 for all domains).

In the case with Talmon's correction: A_{shd} =9, B_{shd}=0.5 and C_{sh}=0.3 for all branches (E_{spir} = 1.0 for all domains), so the standard values of coefficients have been used including similar value of E_{spir} as in DVR approach.

The result is depicted in Figure 9- Figure 11, which shows the magnitude of transverse bed slope (right bank – left bank) along the channel in all domains of the Waal after 10 years of morphological computation. In the region with bend, the transverse slope appears to be steeper in the upper and middle Waal in case of Talmon's correction; whereas the effect is opposite in the lower Waal. It should be noted that one value for A_{shd} has been used for all domains in DVR approach.

2.2.2 Case study for the IJssel model

The values for the parameters for the IJssel models:

In reference computation: A_{sh} = 1.5, 1.1, 0.7 and 0.7 for branch 1, 2, 3 and 4 respectively; B_{sh}=0.5 and C_{sh}=0 for domains (E_{spir} = 1 for all domains). For the reference case, we have carried out simulations using E_{spir} = 1.3 (similar to the case with Talmon's correction) as well, referred to as 'DVR approach with corrected E_{spir}'.

In the case with Talmon's correction: A_{sh} =9, B_{sh}=0.5 and C_{sh}=0.3 for all domains (E_{spir} = 1.3 for all domains).

A comparison on transverse slope (bed level difference between right and left part of the channel) for all the cases and all the domains of the IJssel branch is depicted in Figure 12 - Figure 19Figure 12 (the morphological computation time is indicated in the figure captions). The transverse slope seems to be less steep in Talmon's approach for the first and second domains (Figure 12 and Figure 13); whereas the effect is vice versa for the third and fourth domains (Figure 14 and Figure 15). Similar comparison has been made including the result with higher value of E_{spir} (=1.3) for the DVR approach, which shows the steeper transverse slope for all the domains (which is obvious as the value of E_{spir} is larger).

Given the results, it can be inferred that the value of E_{spir} should be less than 1 for the first and second domains; whereas for the third and fourth domains, the value of E_{spir} between 1 and 1.3 would be appropriate. Obviously, this conclusion is based on the performance of the slope coefficient that includes the relative grain-size and standard value of the coefficients (as proposed by Talmon). In order to identify the correct approach, we need to verify the results of both approaches with the observed data (which is beyond the scope of this study, and could be the part of future work).

2.2.3 Preliminary conclusion

The slope correction including the effect of the relative grain-size appears to be working properly, and can be used in future studies with DVR model and for other morphological studies. The case studies have thrown some light on the effect of slope correction considering relative grain-size as well as its consistency with the approach of calibrating the correction parameters for each domain that is being considered in most morphological studies so far. Obviously, this is relevant only in case of spatially varied grain-size. The effect of the slope correction with relative grain-size on graded sediment transport has not been evaluated in this study, and recommended to be done in future works.

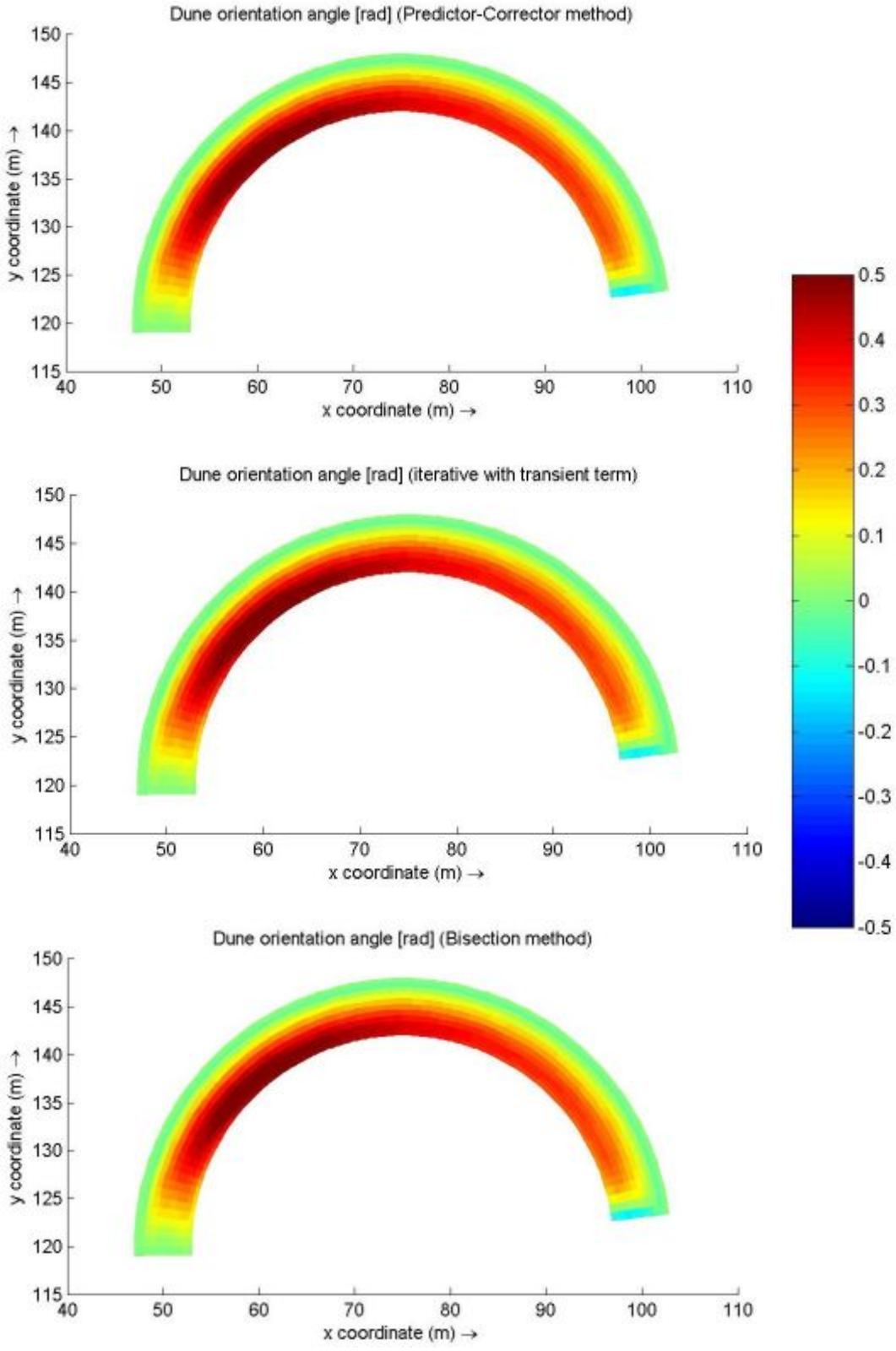

Figure 3 Computational result of dune orientation angle for a curved channel using three different schemes for solution.

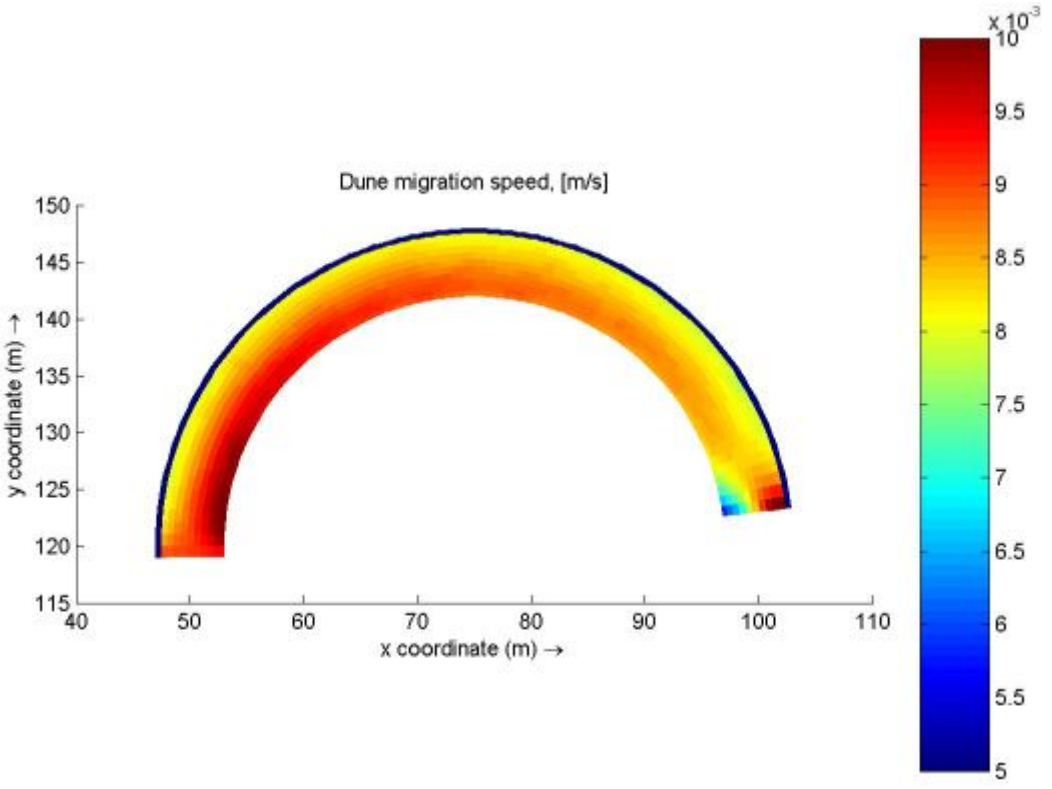

Figure 4 Spatial variation of dune migration speed

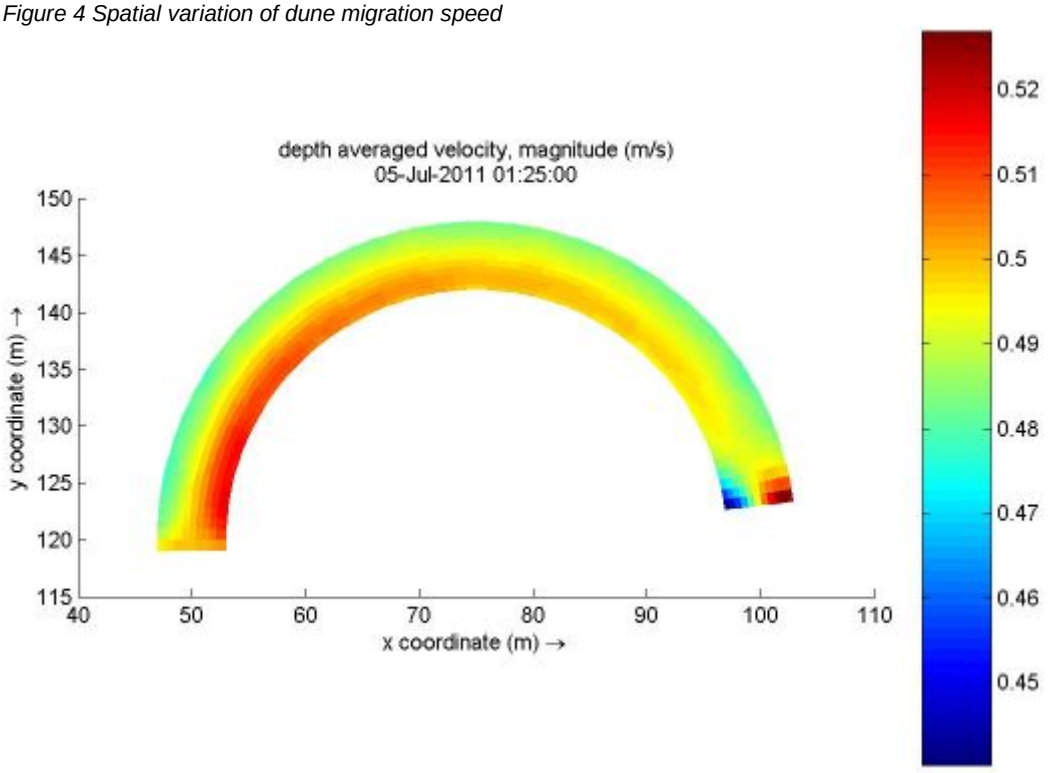

Figure 5 Spatial variation of depth-averaged velocity magnitude

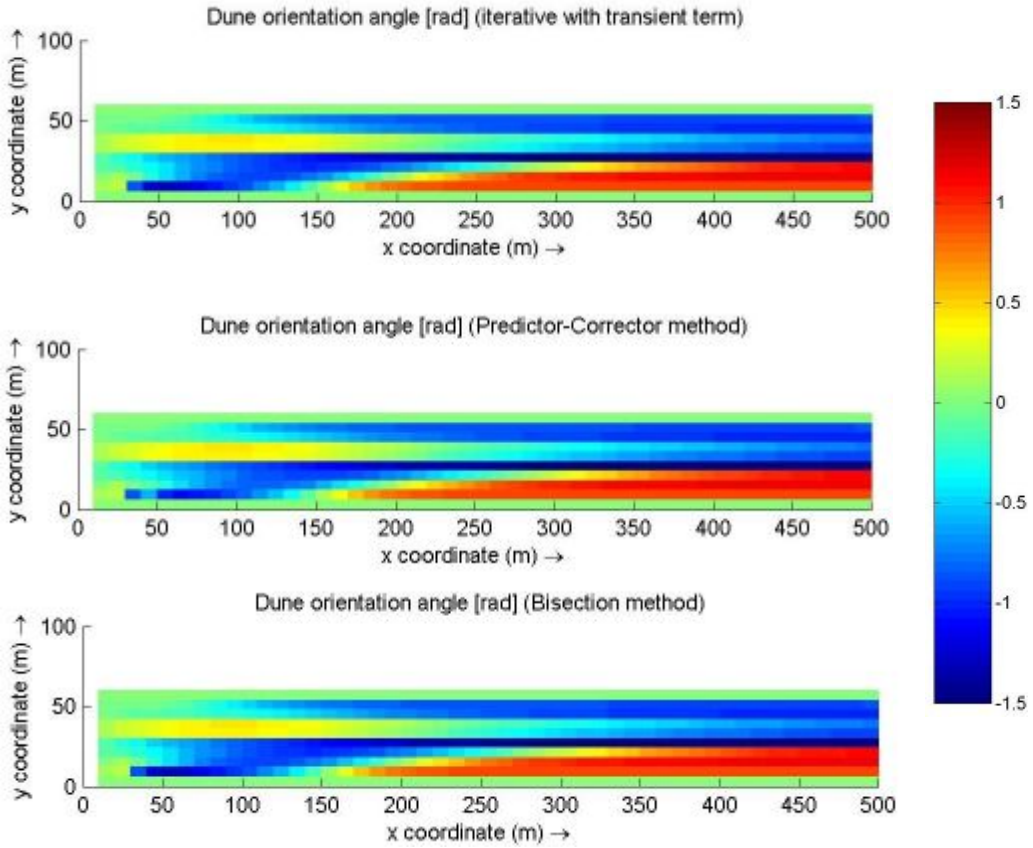

Figure 6 Computational result of dune orientation angle for a straight channel using three different schemes for solution.

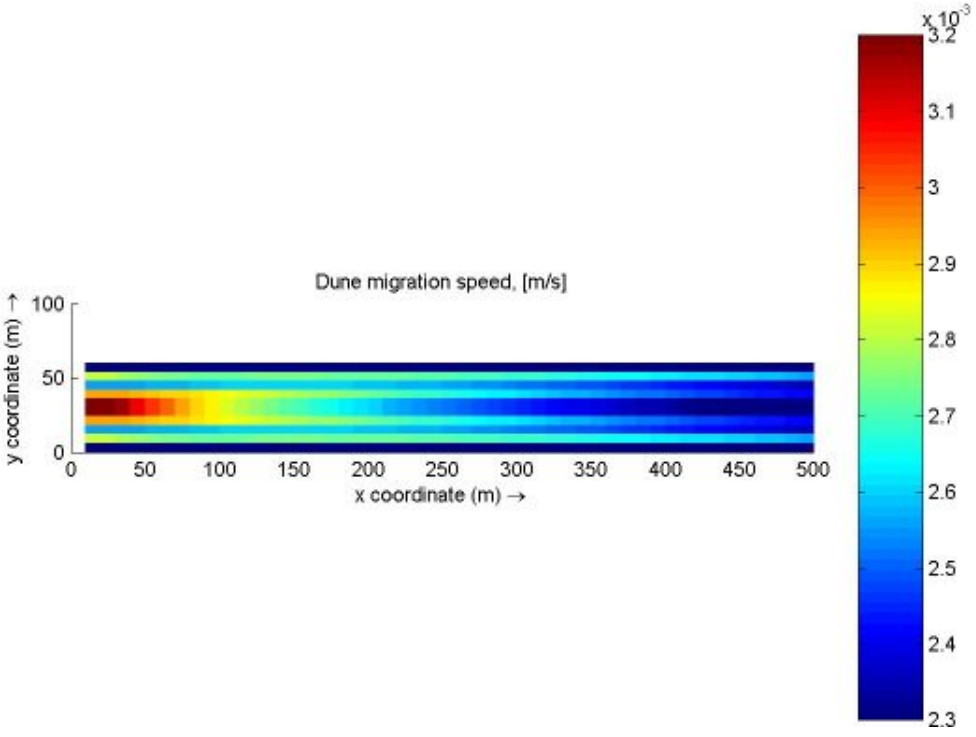

Figure 7 Spatial variation of dune migration speed

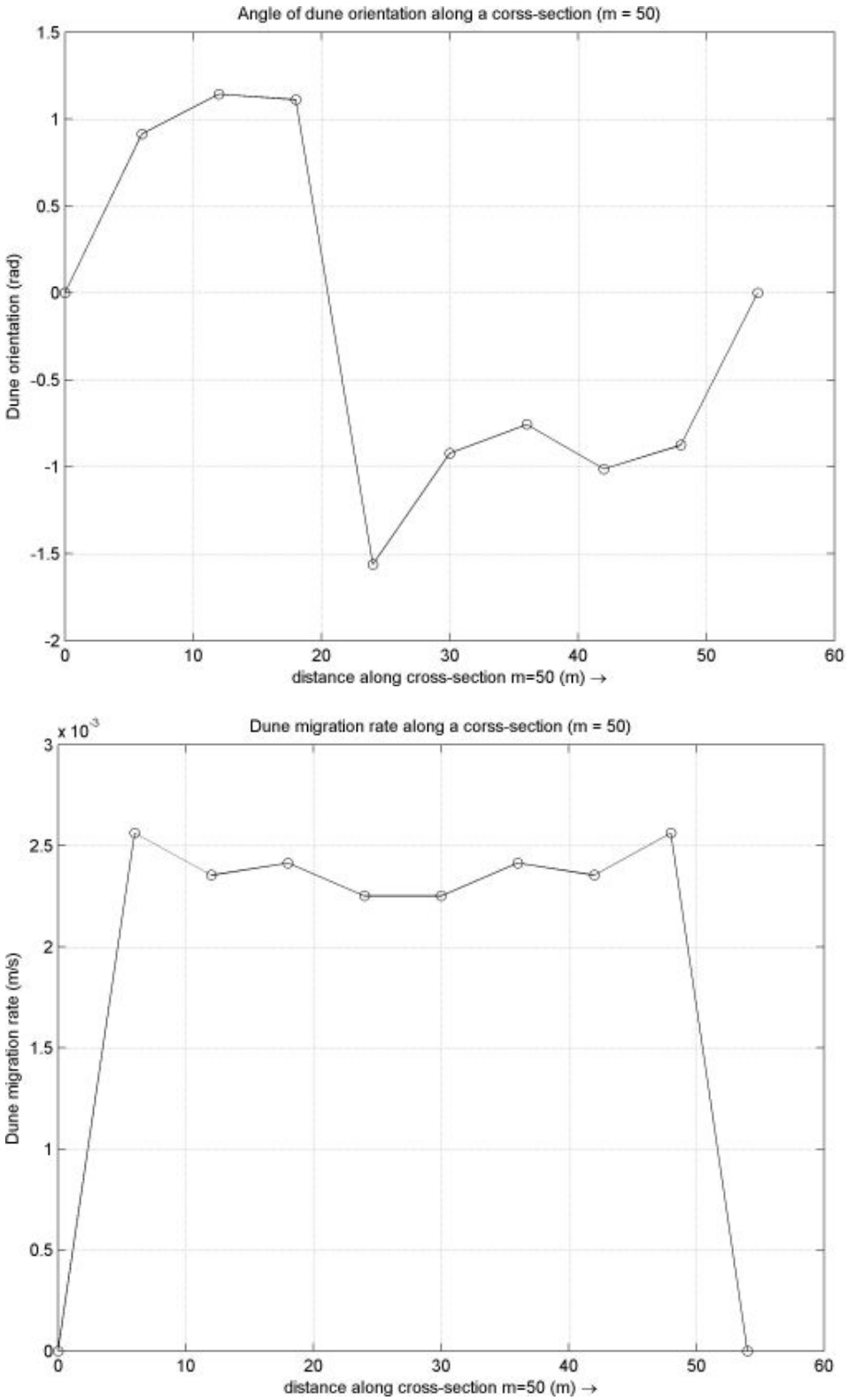

Figure 8 Dune orientation (upper plot) and corresponding migration rate along a selected cross-section of straight channel (m=50)

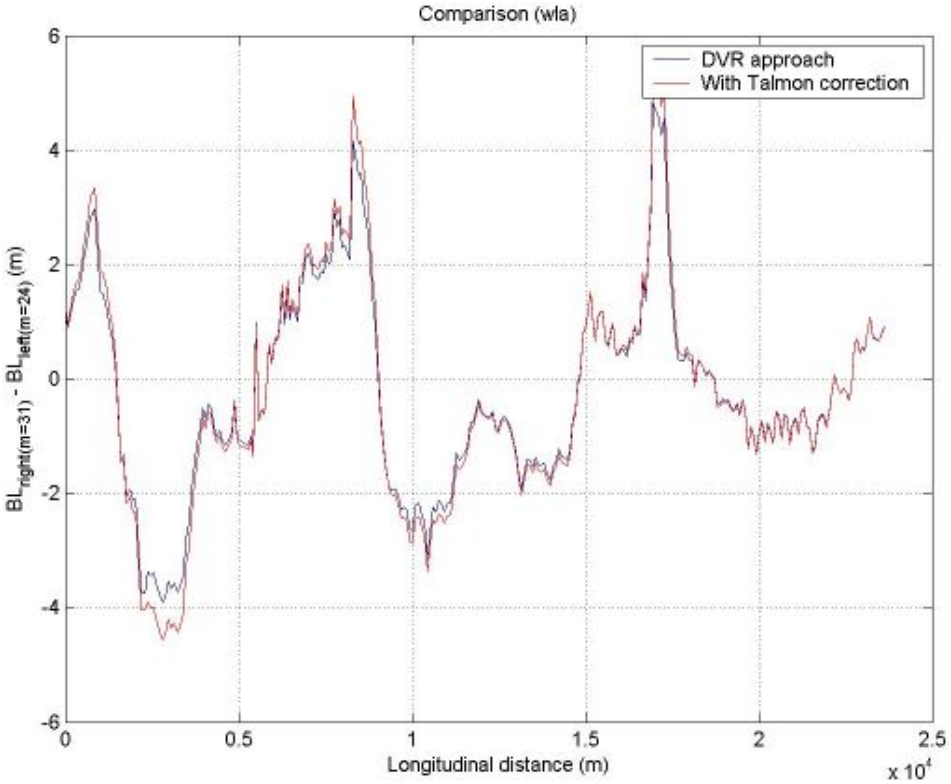

Figure 9 The difference in bed level between right and left banks (indicating the transverse slope; negative value shows opposite slope due to the change in bend direction) for the domain wla (simulation time ~10 years).

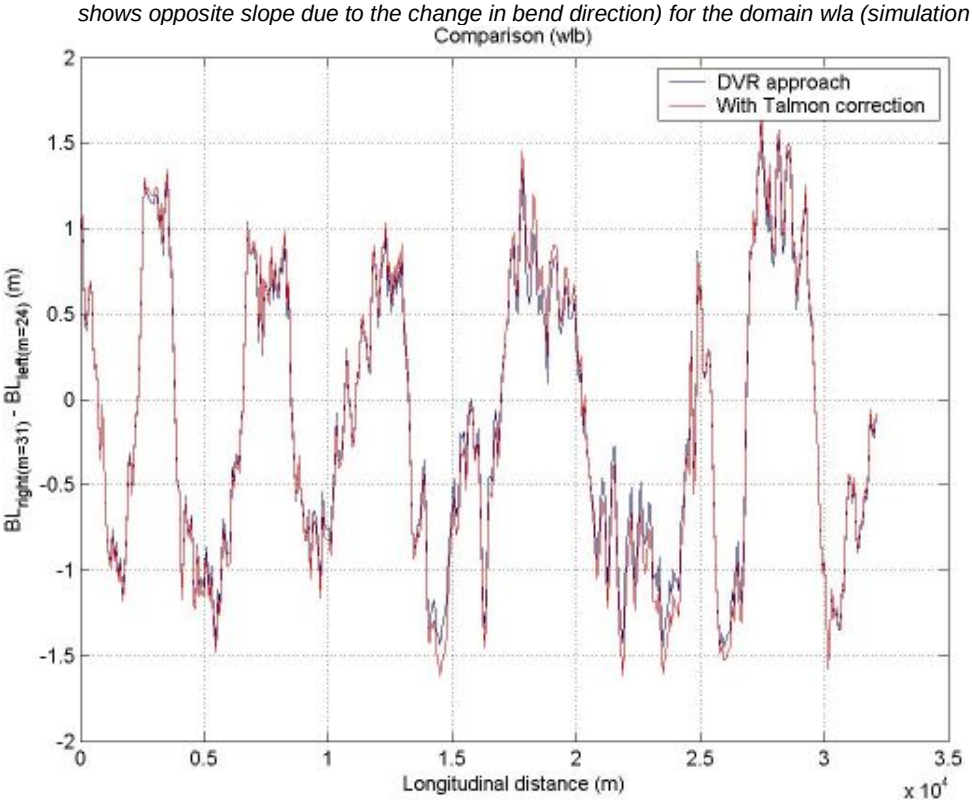

Figure 10 The difference in bed level between right and left banks (indicating the transverse slope; negative value shows opposite slope due to the change in bend direction) for the domain wlb (simulation time ~10 years).

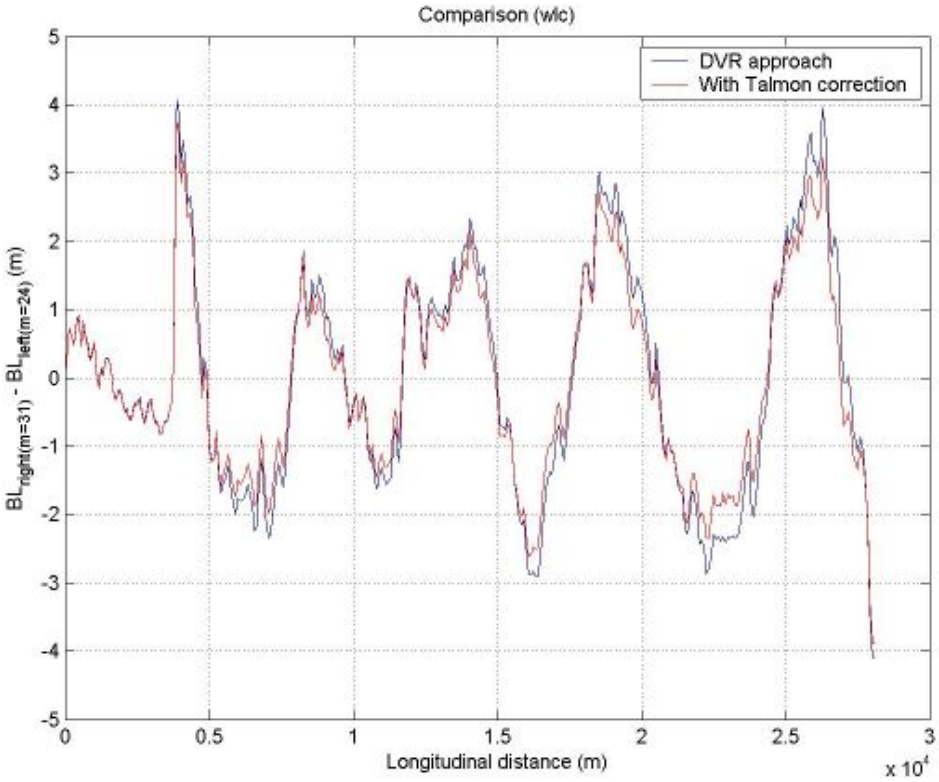

Figure 11 The difference in bed level between right and left banks (indicating the transverse slope; negative value shows opposite slope due to the change in bend direction) for the domain wlc (simulation time ~10 years).

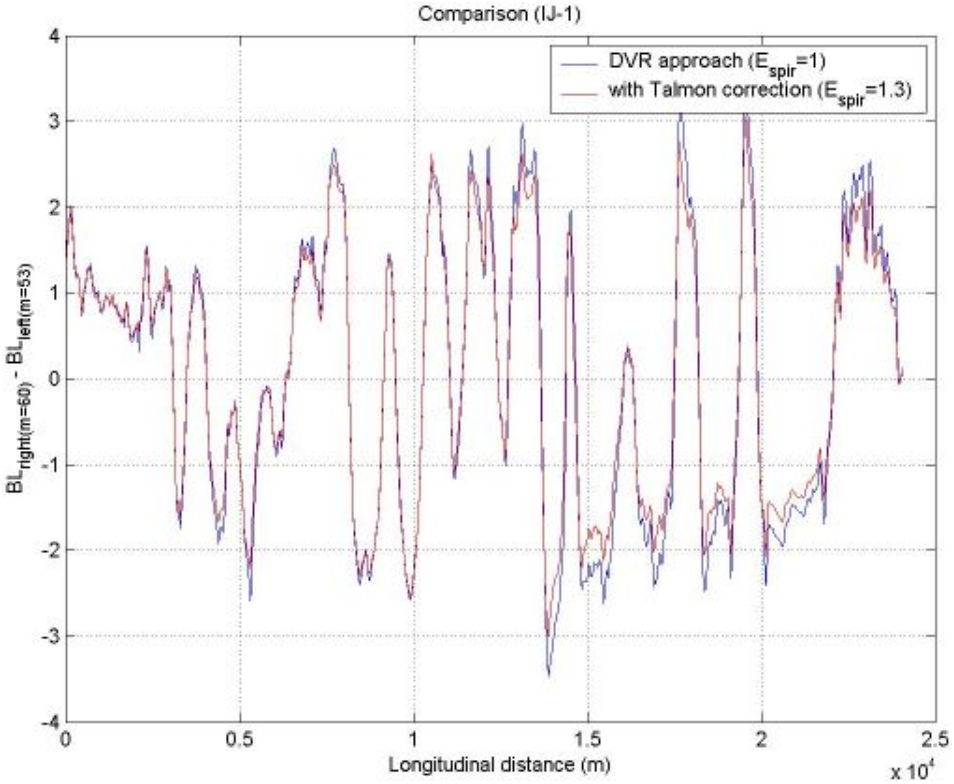

Figure 12 The difference in bed level between right and left banks (negative value shows opposite slope due to the change in bend direction) for the first domain IJ-1 (simulation time ~35 years).

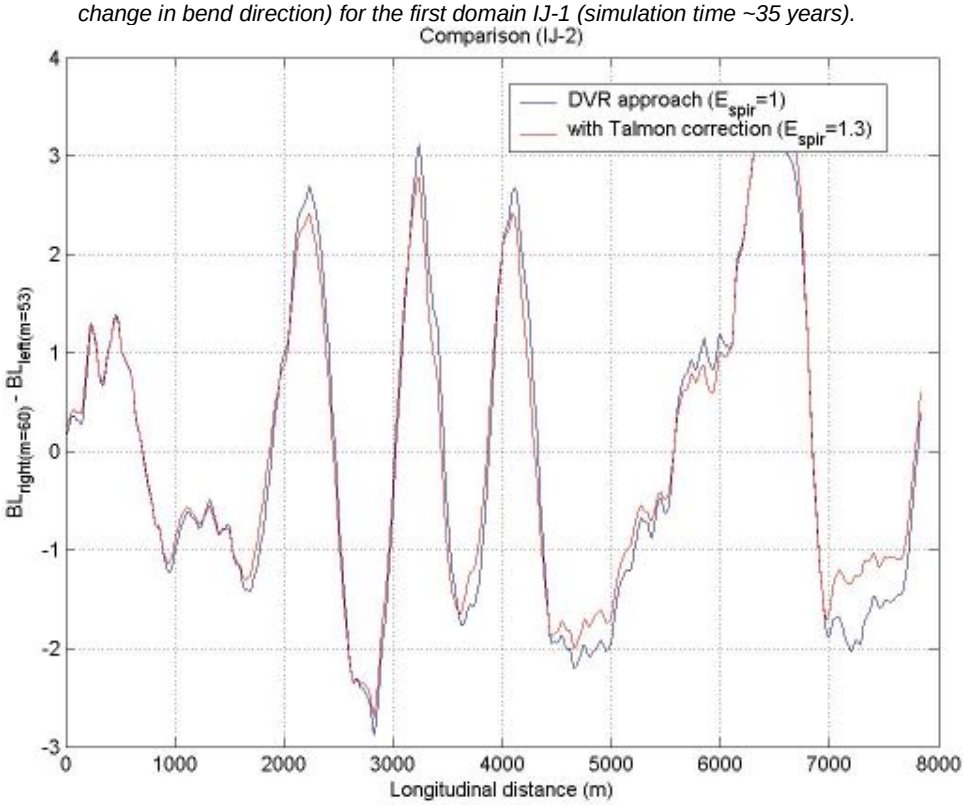

Figure 13 The difference in bed level between right and left banks (negative value shows opposite slope due to the change in bend direction) for the second domain IJ-2 (simulation time ~35 years).

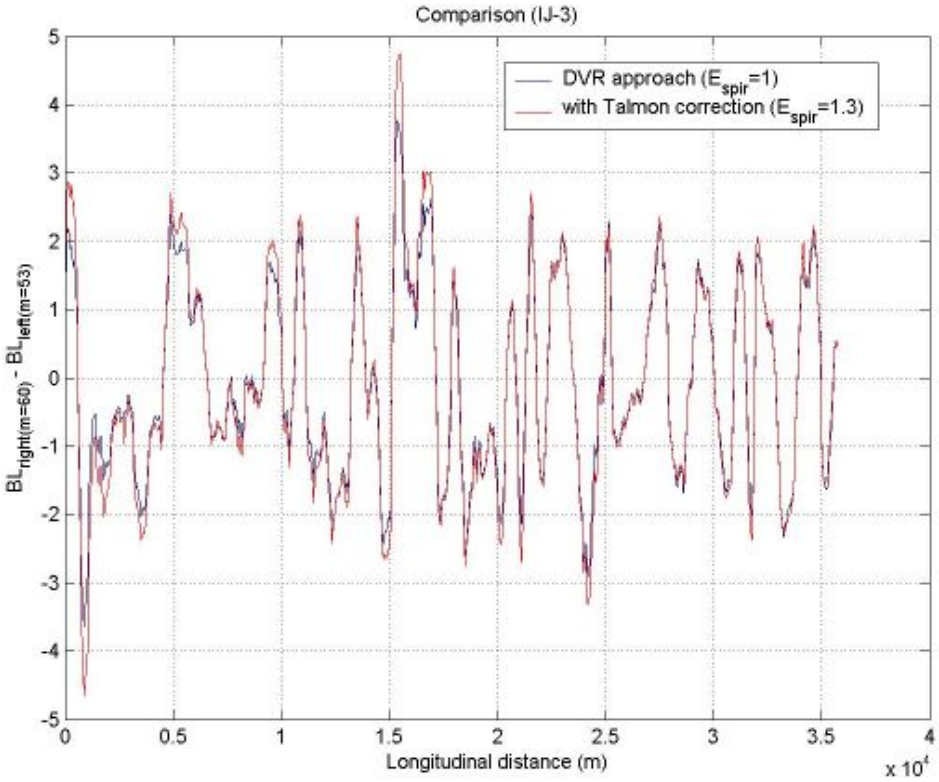

Figure 14 The difference in bed level between right and left banks (negative value shows opposite slope due to the change in bend direction) for the second domain IJ-3 (simulation time ~35 years).

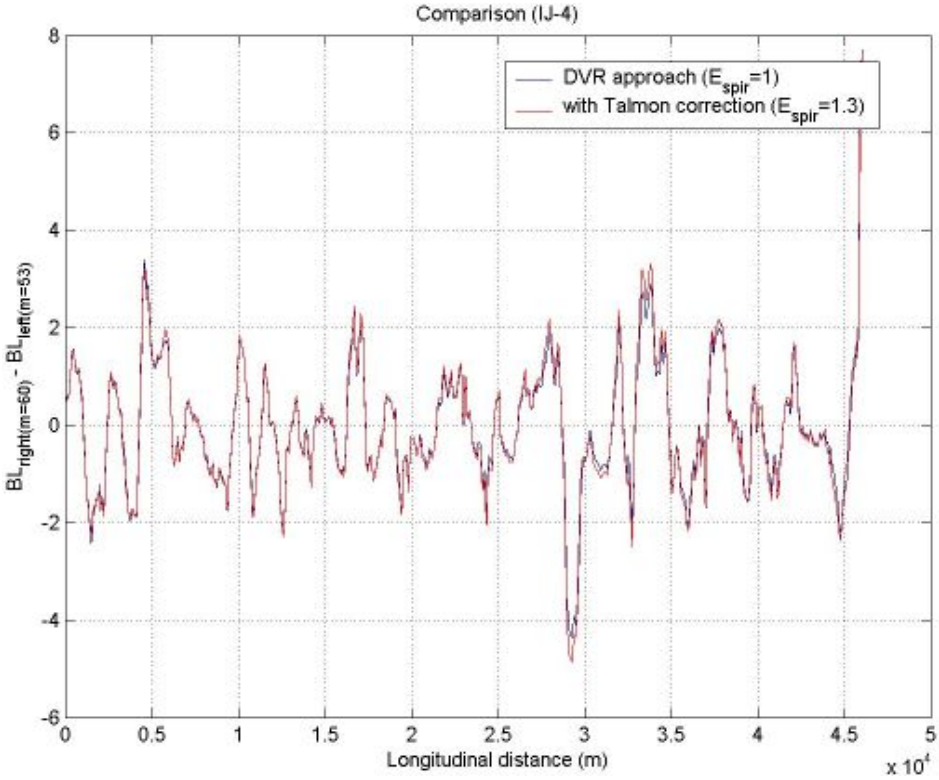

Figure 15 The difference in bed level between right and left banks (negative value shows opposite slope due to the change in bend direction) for the second domain IJ-4 (simulation time ~35 years).

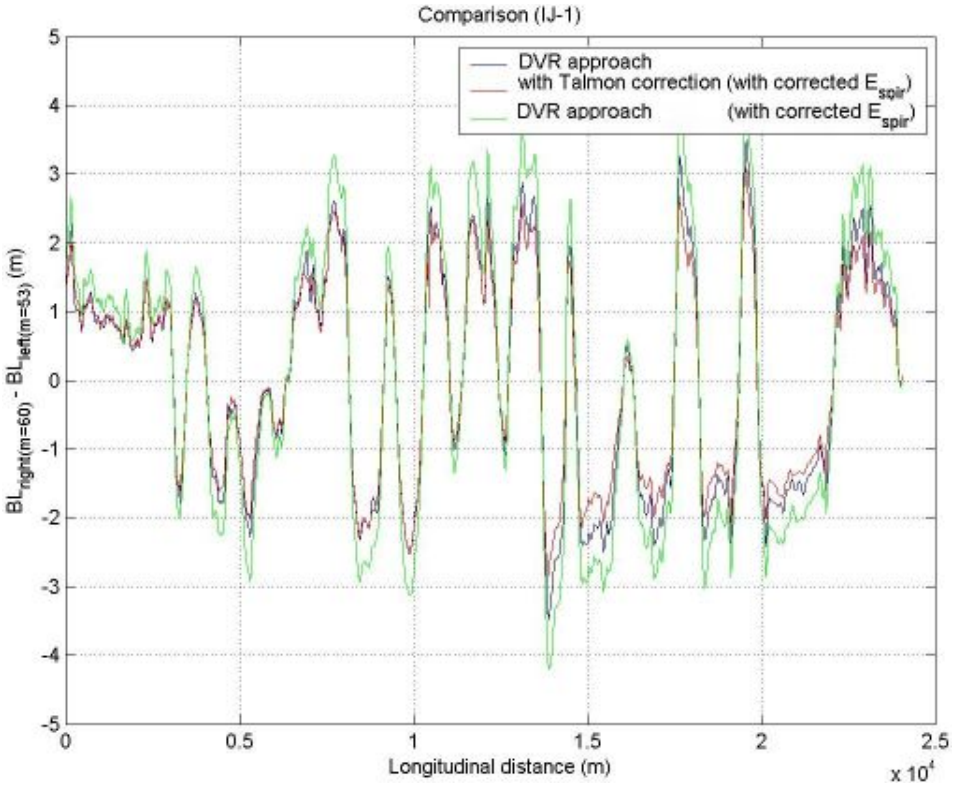

Figure 16 The difference in bed level between right and left banks (negative value shows opposite slope due to the change in bend direction) for the second domain IJ-1 (simulation time ~3 years).

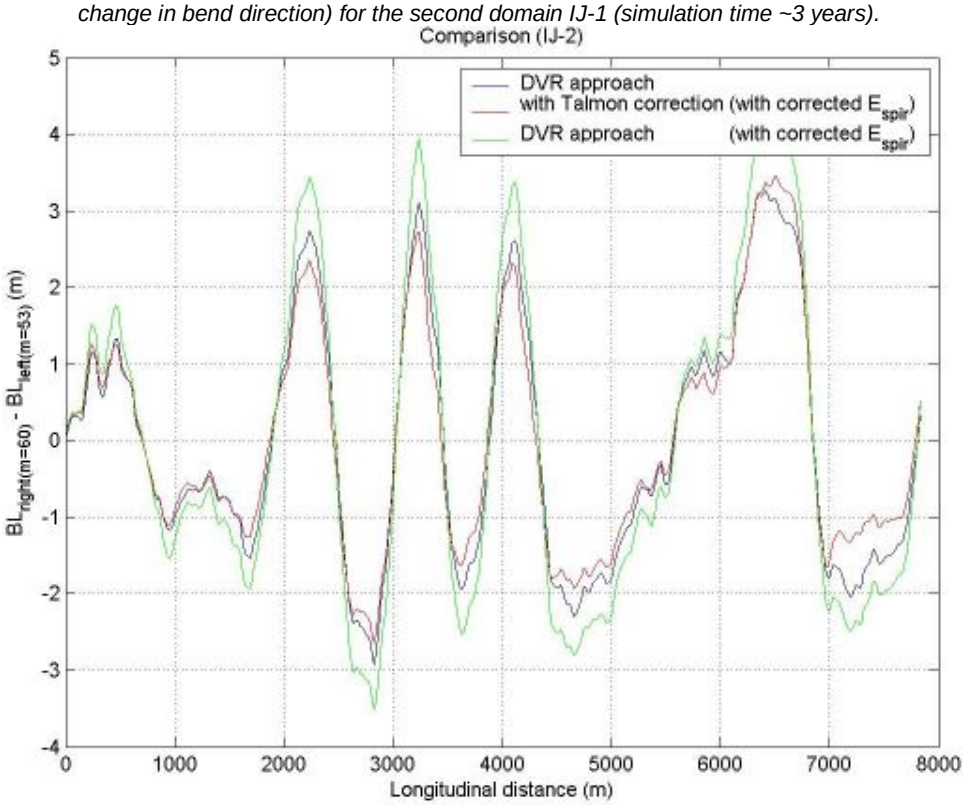

Figure 17 The difference in bed level between right and left banks (negative value shows opposite slope due to the change in bend direction) for the second domain IJ-2 (simulation time ~3 years).

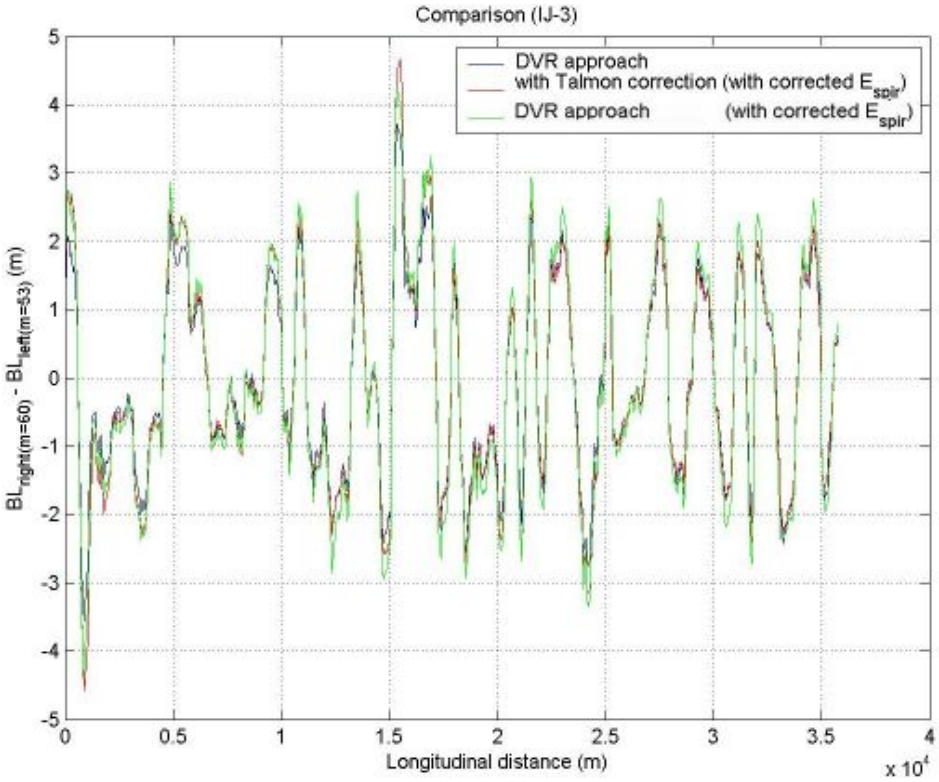

Figure 18 The difference in bed level between right and left banks (negative value shows opposite slope due to the change in bend direction) for the second domain IJ-3 (simulation time ~3 years).

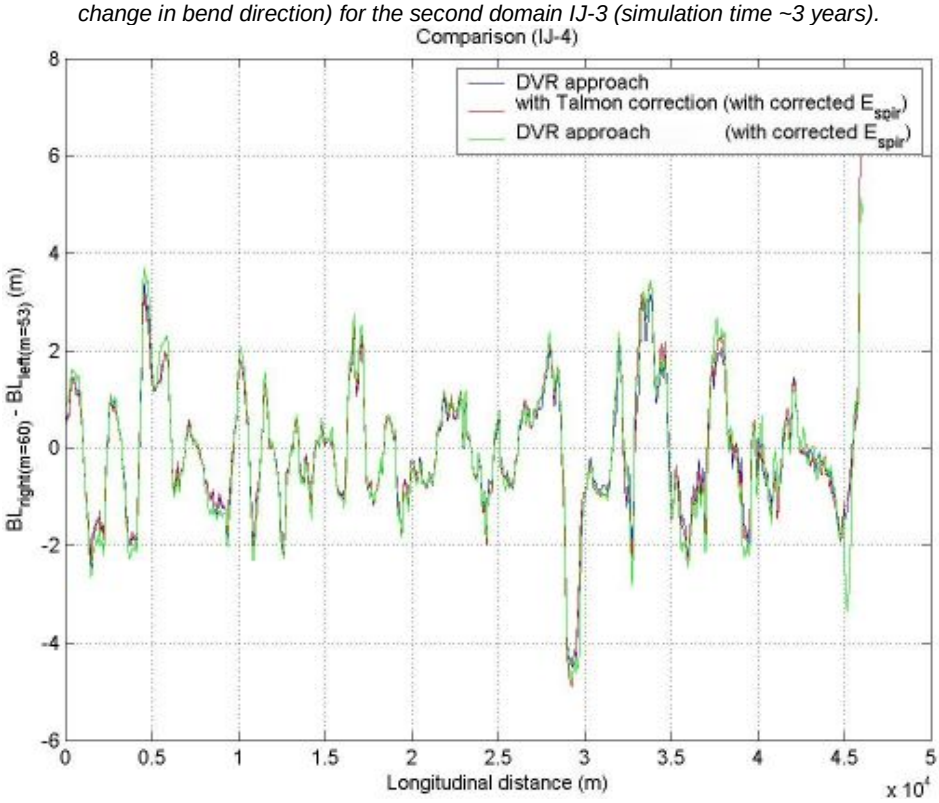

Figure 19 The difference in bed level between right and left banks (negative value shows opposite slope due to the change in bend direction) for the second domain IJ-4 (simulation time ~3 years).